J Low Temp Phys (2012) 167:292–304
DOI 10.1007/s10909-011-0448-8

Kinetic Inductance Detectors

Jochem Baselmans

Received: 25 July 2011 / Accepted: 1 December 2011 / Published online: 20 January 2012

Abstract Microwave kinetic Inductance Detectors, MKIDs, combine device simplicity, intrinsic multiplexing capability and a good sensitivity for radiation detection from the X-ray to the sub-mm part of the electromagnetic spectrum. As a consequence MKIDs are now being developed in several varieties and for many different applications. The paper will shortly address the fundamentals of the physics of MKIDs and will elaborate on the various applications of MKID arrays currently under development.

Keywords Kinetic Inductance Detectors · Superconducting radiation detectors

1 Introduction

The kinetic inductance is the inductance of a material caused by the inertia of its charge carriers. In a superconductor two types of charge carriers are present: Cooper pairs, paired electrons that carry a current without any resistance and quasiparticle excitations [1], whose charge transport is resistive. At low temperatures $T \ll T_c$ the quasiparticle concentration is exponentially small, and the surface impedance of the superconductor is dominated by the kinetic inductance due to the inertia of the Cooper pairs. The kinetic inductance is temperature dependent and it is possible to use the kinetic inductance to measure temperature changes in thin superconducting films [2]. This enables bolometric radiation detection which was originally proposed by McDonald in 1987 [3]. In 2002 it was realized by Zmuidzinas et al. [4] and Sergeev et al. [5] that it is possible to make a much more sensitive radiation detector if changes in kinetic inductance are measured at very low temperatures, typically $T = T_c/10$. One uses the fact that the change in complex surface impedance of a superconducting film

J. Baselmans (✉)
SRON Netherlands Institute for Space Research, Sorbonnelaan 2, 3584 CA Utrecht, The Netherlands
e-mail: J.Baselmans@sron.nl

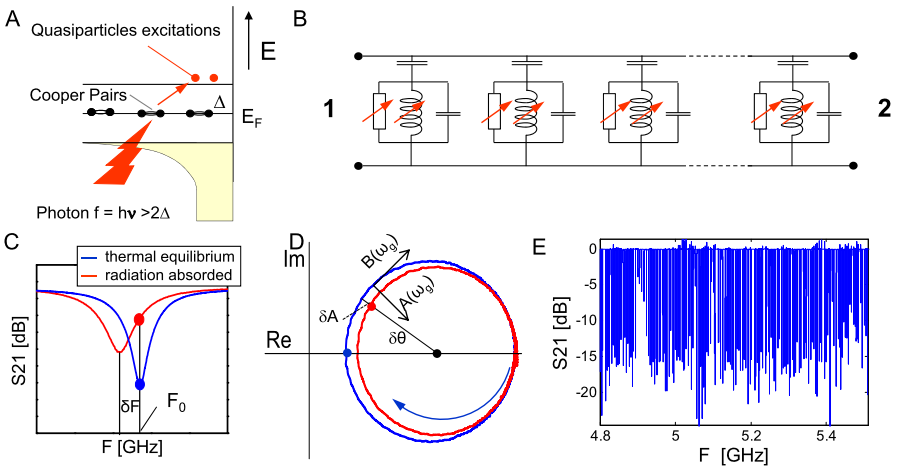

Fig. 1 (Color online) MKID operation principle. **A**: Photons break Cooper pairs in a superconductor creating quasiparticles. **B**: By making the superconductor part of a resonance circuit it is possible to read out changes in the complex surface impedance of the superconductor due to radiation absorption as a change in microwave transmission. Frequency division multiplexing can be achieved by coupling many resonators to 1 feedline. **C**: Measured transmission from contact 1 to 2 in **B** for 1 resonator. The *blue line* represents the equilibrium situation and the *red line* after photon absorption. **D** shows the same data as in **C** but in the complex plane, showing that either δA or $\delta\theta$ using a readout tone at F_0 can be used to measure the amount of absorbed radiation. The *arrow* indicates the direction of increasing frequency, $B(\omega_g)$ and $A(\omega_g)$ represent the direction tangent and normal to the resonance circle. **E**: 175 resonators with $Q = 2 \cdot 10^4$ and $\delta F_0 = 4 \pm 2$ MHz

per quasiparticle $\delta Z_s / \delta N_{qp}$ is *independent* of temperature. So one operates the device in thermal non-equilibrium: the quasiparticles are excess particles created by radiation absorption decaying over time. Sergeev et al. [5] proposed a detector where the changes in bias current in a small superconducting circuit are measured by a SQUID. A more elegant method was proposed by J. Zmuidzinas et al. [4] and worked out further in [6]. The idea was to use a superconducting thin film microwave resonator to detect changes in the surface impedance of the superconducting film by detecting changes in properties of the resonance circuit: the microwave kinetic inductance detector, MKID. This is a very powerful and elegant concept which is explained below.

2 MKID Principle of Operation

A MKID is a superconducting pair breaking detector, where the fundamental radiation absorption mechanism is the creation of quasiparticle excitations in a superconducting material. This is illustrated in Fig. 1A where I give the semiconductor representation of a superconducting material at very low temperatures. The Cooper pairs are represented as paired particles at the Fermi energy E_F, the quasiparticles are represented as single particles at energies $E \geq E_F + \Delta$, where Δ is the energy gap of the superconductor. A photon with an energy $h\nu > 2\Delta$ incident on the superconducting film can be absorbed by breaking up Cooper pairs and creating a number

of quasiparticle excitations $N_{qp} = \eta h\nu/\Delta$, with $\eta \approx 0.59$ the efficiency of creating quasiparticles [7]. The change in quasiparticle number changes the complex surface impedance of the superconductor $Z_s = R_s + i\omega L_s$, where R_s is a resistive term associated with the quasiparticles, and L_s the kinetic inductance due to the Cooper pairs. The change in surface impedance δZ_s is read out by making the superconducting film part of a resonant circuit loading a microwave transmission line, referred to as feedline. An equivalent circuit is given in Fig. 1B, where the variable inductor and variable resistor represent the superconducting film. At low temperatures $T \ll T_c \omega L_s \gg R_s$, resulting in negligible losses in the resonance circuit. As a result the internal Q factor of the resonator, which is determined by the losses in the system, can be as high as 10^7. On resonance the circuit shorts the transmission line with the result that we observe a strong decrease in transmitted power from contact 1 to 2. This is indicated for one resonator in Fig. 1C by the blue line tracing the deepest resonance dip. For a MKID the resonance frequency F_0 is a typically a few GHz, the Q factor, determined by the coupling to he feedline and the losses, is of the order of 10^4–10^6 and the resonator bandwidth $\mathrm{BW} = F_0/Q$ is of the order of 10^4–10^5 Hz. The absorption of a photon will cause the resonance center frequency to shift to lower values and the resonance dip to decrease in depth. This is indicated in Panel C by the red line. The MKID can be readily read-out by using a single tone at the resonance frequency of the device at thermal equilibrium. Radiation absorbed results in a reduction in transmitted magnitude, as shown by the two dots in Panel C. In the complex plane the resonance feature traces a circle, as shown in Fig. 1D, and the absorption of radiation causes a phase change $\delta\theta$ and a change in radius δA. Using $\delta\theta$ is typically referred to as phase readout and using δA is referred to as amplitude or dissipation readout. A MKID array can be read-out using frequency domain multiplexing in the GHz domain by coupling many resonators with a slightly different resonance frequency, as shown in Fig. 1B, E. Typically a resonance frequency spacing of 1–2 MHz is achievable, allowing 2–4 thousand pixels to be read out using one 4 K low noise amplifier with a bandwidth of 4–8 GHz and two coaxial cables connected to ports 1 and 2 of the feedline.

3 Sensitivity Limits

A MKID is a superconducting pair breaking detector. In thermal equilibrium the intrinsic sensitivity is limited by the random thermal generation and recombination of quasiparticles. This results in a sensitivity limit expressed in the generation-recombination noise equivalent power, NEP_{G-R},

$$\mathrm{NEP}_{G-R} = \frac{2\Delta}{\eta}\sqrt{\frac{N_{qp}}{\tau_{qp}}} \propto \exp\left(-\frac{\Delta}{k_B T}\right) \tag{1}$$

with N_{qp} the quasiparticle number and τ_{qp} the quasiparticle lifetime. Clearly operating a MKID at a temperatures well below the critical temperature will result in an exponentially low NEP_{G-R}. This is valid only as long as the quasiparticle number and

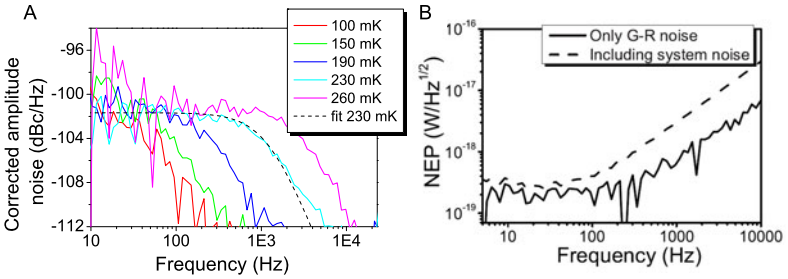

Fig. 2 (Color online) **A**: Measured amplitude noise spectral density of a 50 nm thick 1/4 λ coplanar waveguide aluminium MKID as a function from temperature with setup noise subtracted as presented in [11] and [13]. The temperature independent noise level and temperature dependent are an unambiguous signature of generation-recombination noise. **B**: NEP_{G-R} and the NEP also including system noise contributions at 100 mK. Data from [11]. © American Physical Society

quasiparticle lifetime follow their theoretical exponential dependency with temperature [8]. The noise power spectral density of a MKID resonator due to quasiparticle number fluctuations S_{G-R} can be expressed as [9–11]

$$S_{G-R} = \frac{4N_{qp}\tau_{qp}}{1+(\omega\tau_{qp})^2} \cdot \left[\frac{\delta(A,\theta)}{\delta N_{qp}}\right]^2 \tag{2}$$

where $\delta(A,\theta)/\delta N_{qp}$ represents the amplitude or phase change per quasiparticle (see Fig. 1A). The first term in (2) represents the power spectral density of the quasiparticle number noise. As demonstrated by Wilson et al. [9, 10] the amplitude of this signal, $4N_{qp}\tau_{qp}$ is constant with temperature, the increase in the total noise power spectral density only manifests itself as an increase of the bandwidth of the noise signal, described by $(1+(\omega\tau_{qp})^2)^{-1}$. So as long as the KID responsivity $\delta(A,\theta)/\delta N_{qp}$ remains constant, generation-recombination noise limited performance of a MKID detector is associated with a temperature independent noise level with a temperature dependent Lorenztian roll-off of the spectrum. This was recently observed using amplitude readout of an Al λ/4 coplanar waveguide resonator in a well controlled light-tight setup [12] by Visser et al. [11, 13], the results are reproduced in Fig. 2A. From the data the authors are able to determine the quasiparticle density and lifetime as a function of bath temperature. At higher temperatures $T > 180$ mK they observe $\tau_{qp}, N_{qp}^{-1} \propto \exp\Delta/(k_B T)$ as expected. At $T < 160$ mK τ_{qp}, N_{qp} saturate to a constant value that depends on the readout power [13]. The authors estimate $\mathrm{NEP}_{G-R} = 2 \cdot 10^{-19}$ W/$\sqrt{\mathrm{Hz}}$ at $T = 100$ mK, limited by the excess quasiparticle number and shown in Fig. 2B.

In the case of a practical MKID detector the sensitivity limit depends not only on the generation-generation noise, but depends also on the photon energy, photon arrival rate and device time constant. Two main limits can be considered: Single photon counting, where the arrival rate of photons is smaller than the device bandwidth, and photon integration, where the photon arrival rate is so fast that the device measures a time average flux. In the case of single photon detection, typical for cryogenic optical, UV and X-ray detectors, one is typically interested to obtain the photon energy.

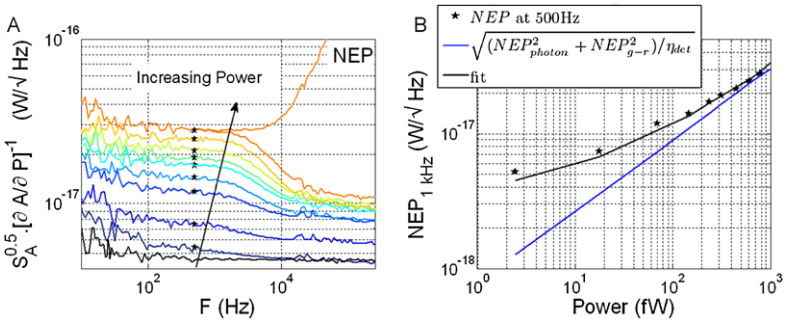

Fig. 3 (Color online) **A**: The measured $S_R^{0.5} \cdot [dA/dP]^{-1}$ as a function of loading power. This parameter has the same spectral shape as the noise and is identical to the devices NEP at frequencies blow the quasiparticle roll-off, the real NEP is included for the highest loading power. At higher loading powers a white noise spectrum with a roll-off at 1.5 kHz dominates the noise from the amplifier, given by the *lowest* (*black*) *line*. The measured NEP at 500 Hz is plotted in panel *B* as function of loading power. It asymptotically approaches the photon noise limit as shown by the *blue line*. Reproduced from [16], © American Institute of Physics

The energy resolution ΔE for any pair breaking detector is given by the Fano limit as:

$$\Delta E = 2.355\sqrt{E_{photon}\Delta F \eta^{-1}} \tag{3}$$

with F the Fano factor, which for Ta is given by $F = 0.22$. This results in $E/\Delta E \approx = 30$ for $\lambda = 1$ μm absorbed in a Ta absorber. To reach this energy resolution a NEP $\approx 4 \cdot 10^{-19}$ W/$\sqrt{\text{Hz}}$ is required, indicating that Fano limited performance in the near-IR requires very sensitive detectors.

In the case of photon integration the sensitivity is limited by the random arrival rate of photons. The associated photon noise limited NEP due to a power absorbed P with a photon frequency ν is given by

$$\text{NEP}_{photon} = \sqrt{2Ph\nu(1 + mB)} \simeq \sqrt{2Ph\nu} \tag{4}$$

The $(1 + mB)$ term is the correction to Poisson statistics due to wave bunching [14]. For a pair breaking detector such as a MKID the absorbed power creates a number of quasiparticles

$$N_{qp} = \frac{P\tau_{qp}}{\eta\Delta} \tag{5}$$

The larger number of quasiparticles, and resulting reduction in quasiparticle lifetime $\tau_{qp} \propto 1/N_{qp}$ increases NEP_{G-R} according to (1). However, the exact generation-recombination noise under loading is not easy to calculate: The quasiparticle generation is not a thermal process but correlated with the photon arrival, η depends on the photon energy if the photon energy becomes of the order of the energy gap and the readout current can also create quasiparticles. See [15] for a detailed discussion. In the high loading limit, where effectively all quasiparticle are created

by the loading power, one can approximate the NEP of a photon noise limited MKID as [16, 17]

$$\mathrm{NEP}^2 = \left(\mathrm{NEP}^2_{G-R} + \mathrm{NEP}^2_{photon}\right)/\eta_{opt} \simeq \left(\frac{P\Delta}{\eta} + 2Ph\nu\right)/\eta_{opt} \tag{6}$$

with η_{opt} the optical efficiency. Analog to (2) we can approximate the noise power spectral density of a photon noise limited MKID detector:

$$S = \left(S_{G_R} + S_{photon}\right) \simeq \left(\frac{2N_{qp,P}\tau_{qp}}{1+(\omega\tau_{qp})^2} + \frac{2N_{qp,p}\tau_{qp}\eta hf/\Delta}{1+(\omega\tau_{qp})^2}\right)\cdot\left[\frac{\delta(A,\theta)}{\delta N_{qp}}\right]^2 \tag{7}$$

with $N_{qp,p}$ the quasiparticle number due to photon absorption. The reduction by a factor 2 in S_{G-R} is because quasiparticle generation is not a thermal process but correlated by the photon absorption and therefore taken as negligible, leaving only the recombination noise contribution.[1] From (6) and (7) several conclusions can be drawn for a photon noise limited MKID under loading: (a) the noise of the MKID has a white spectrum, rolled off by the quasiparticle lifetime. (b) the noise level is *independent* of the absorbed power and determined by the radiation frequency. (c) the device NEP is always a bit higher than NEP_{photon} due to the contribution from quasiparticle recombination and (d) the total device NEP $\propto \sqrt{P}$ (6). So, for a MKID to reach the photon noise limit the product $N_{qp,p}\tau_{qp}\cdot(\delta(A,\theta)/\delta N_{qp})^2 \propto N_0\tau_0\cdot(\alpha Q/V)^2$ must exceed the amplifier or MKID noise contributions. Here α is the kinetic inductance fraction, τ_0 is the interaction time constant as defined by Kaplan et al. [8] and N_0 is the single spin density of states at the Fermi level. It can be shown that $N_0\tau_0\cdot(\alpha Q/V)^2 \propto b^{-1}\Delta^{-1}\cdot(\alpha Q/V)^2$ with b a material dependent quantity related to the electron-phonon coupling strength [8]. Hence the best material to reach photon noise limited detection is a low T_c superconductor with a high kinetic inductance Fraction that enables high-Q resonator fabrication. High Q factors can be achieved with any superconducting material without a lossy native oxide on a crystalline substrate. Aluminium has been used traditionally and is a good material with one important drawback that it has a small value of α, typically of the order of 10% for CPW resonators. In this context TiN is very promising, it has a large magnetic penetration length and therefore α can be close to unity. The critical temperature can be engineered by changing the material stoichiometry from 4.5 K to 0.8 K and internal Q factors up to 10^7 have been measured [18, 19]. For $T_c \approx 1$ K a dark NEP $\approx 3\cdot 10^{-19}$ W$\sqrt{\mathrm{Hz}}$ has been measured [18].

Recently Yates et al. [16, 17] have measured photon noise limited performance of an antenna coupled MKID as shown in Fig. 7A, the results are reproduced in Fig. 3. In the figure the measured optical NEP spectra are plotted as a function of loading power. The NEP spectra in Fig. 3A are white with a roll-off due to the quasiparticle lifetime, as expected for photon noise limited detection by the MKID. In Fig. 3B the NEP at 500 Hz is plotted as a function of loading power, asymptotically approaching photon noise limited performance as the detector noise contributions become smaller

[1] In the equation presented we approximate the generation-recombination noise as being only due to thermal recombination, and we ignore also any quasiparticle creation due to the readout currents. For a more elaborate discussion we refer to [15].

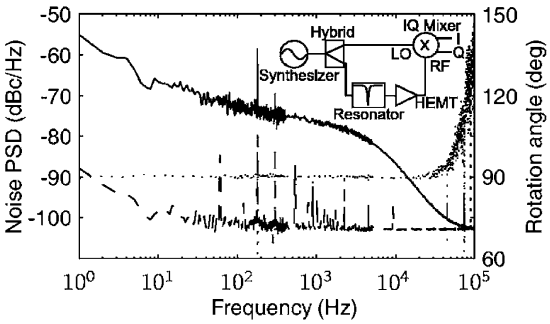

Fig. 4 Typical phase noise (*top line*) and amplitude noise (*bottom line*) of a MKID resonator. Data reproduced with permission from [20], © American Institute of Physics

with increasing loading power. The optical efficiency of the detector was measured using the photon noise level to be 80% for one polarisation, indicating that efficient radiation coupling is possible with an antenna coupled MKID.

4 MKID Excess Noise

The only source of excess noise in MKIDs is frequency noise, which manifests itself in fluctuations tangential to the resonance circle, i.e. in the direction of $B(\omega_g)$ in Fig. 1D. The result is an excess phase noise with respect to the MKID resonance circle, with a frequency dependence as depicted by the top line in Fig. 4 [20]. In the direction perpendicular to the MKID circle (in the direction of $A(\omega_g)$ in Fig. 1D) there is no evidence of noise from the resonator even at levels well below the standard quantum limit [21], i.e. using the amplitude or dissipation readout the noise of an MKID is determined solely by the amplifiers in the readout chain. Using amplitude readout excess phase noise can thus be circumvented as proposed by [20] and demonstrated by [22]. The drawback is the smaller KID responsivity. It was demonstrated by [24, 25] that the excess phase noise is caused by two level systems (TLS) in a thin dielectric surface layer interacting with the electric fields in the resonator. As suggested by ref. [24] and demonstrated by Noroozian et al. [26] the noise can be strongly reduced by making the capacitive section wider while leaving the inductive section of the resonator narrow to prevent deterioration of the device response. Barends et al. [25] demonstrated that NbTiN resonators have lower frequency noise than Al or Ta devices. In [27] it is proven that the dominant noise source in NbTiN resonators is a thin surface layer on top of the Si substrate. By removing the Si the authors further improve the low noise of NbTiN resonators. Further reductions in TLS related noise seem to be possible by using parallel plate capacitors with single crystal dielectrics [28].

5 MKID Types

MKIDs are based upon microresonators with a resonance frequency F_0 of the order of a few GHz. The two main types, coplanar waveguide $\lambda/4$ distributed resonators and lumped element resonators, are depicted in Fig. 5. The $\lambda/4$ resonator consists

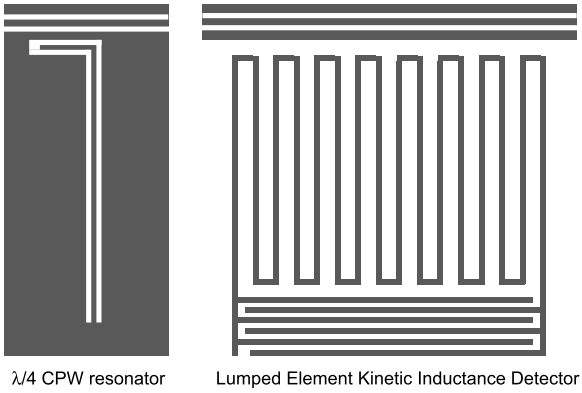

Fig. 5 Two different types of MKID resonators, the dark areas represent the superconducting film, white is bare substrate

of a shorted section of CPW line, with a length $l = c/4F_0 \cdot \sqrt{1/\varepsilon_{eff}}$ (with ε_{eff} the effective dielectric constant of the transmission line) shunt-coupled to a CPW feedline. These CPW resonators are typically fabricated on crystalline substrates, mitigating problems associated with two level systems in non-crystalline dielectrics such as high excess noise and low Q factors [23]. Microstrip resonators are smaller, and recently microstrip resonators with a dielectric made of hydrogen rich amorphous Si (a-Si:H) have shown [29] Q factors close to 10^6. Since a distributed resonator as such is not a detector, a separate structure is required to couple efficiently to the radiation. Also quasiparticles need to be created and confined to the inductive section of the resonator [30].

A very elegant resonator geometry, that combines a resonator and radiation detector in one planar structure, was proposed by Doyle et al. in 2008 [31] by the lumped element kinetic inductance detector, LeKID. The LeKID consists of a meandering inductor and interdigital capacitor coupled to a feedline. Sub-mm radiation can be absorbed very efficiently by the inductor by illuminating the backside of the chip and using backshorts and well defined chip layer thicknesses to create an absorbing cavity. The important challenge for LeKIDs is that the material parameters determine the properties of the resonator but also determine the radiation absorption efficiency. Aluminium has a very low resistivity, which makes efficient radiation absorption difficult. TiN films have a much higher resistivity than Al and are therefore ideally suited to make LeKIDs. Additionally sub-stoichiometric TiN with a low nitrogen content is grey, and therefore has reasonable quantum efficiencies for optical and IR photons [40]. An interesting variation to the standard LeKID geometry is the one proposed by Brown et al. [32] where the MKID is formed of a parallel plate transmission line, using a 1.5 μm thick crystalline Si membrane from a SOI wafer as the dielectric.

6 Applications and Instruments

Several instruments for mm-wave astronomy, sub-mm astronomy and optical astronomy are currently being developed by US and European groups and demonstration instruments have been successfully tested at various observatories. MUSIC is

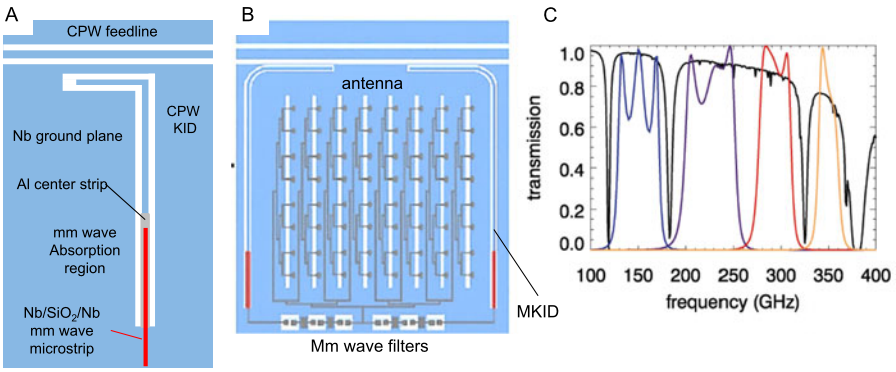

Fig. 6 (Color online) **A**: Schematic representation of a Nb resonator with Al section for mm wave absorption (after [34]). The mm wave radiation travels through the Nb stripline and is absorbed in the Al section. **B**: Schematic of a 2 color pixel, similar in concept as the final 4 color pixel from MUSIC (reproduced from [34]). **C**: Transmission of the 4 mm wave filter banks for MUSIC (reproduced from [33])

a 756 pixel, mm-wave multicolor instrument developed by a US consortium for the Caltech Sub-millimeter Telescope in Hawaii [33]. The KID array design, as shown in Fig. 6 uses a large broad band phased array antenna to couple radiation into a microstripline. Using on chip microstrip LC filters, the mm wave signal is split into 4 striplines, each corresponding to a narrow frequency band signal (Fig. 6C). The radiation of each band is absorbed in a separate MKID by running the mm-wave stripline over the Al center line of the $1/4\lambda$ CPW resonator. The Al line is the last section of the central line of the resonator, which for the rest is made from Nb. The low gap frequency of Al ($\simeq$80 GHz) allows quasiparticle creation and the Nb with a gap frequency of $\simeq$650 GHz remains lossless for the 100–400 GHz band of the instrument. The instrument is thus capable of 4-color detection with each spatial pixel. Several engineering runs have been performed, with increasing instrument sensitivities [34], with noise equivalent flux densities of several hundred mJy $s^{1/2}$. The instrument is read out using the 550 MHz open-source digital electronics described in [35].

NIKA is a European instrument being developed for the IRAM 30 m telescope in Granada, Spain [36, 37]. NIKA is a dual band imaging instrument with two separate arrays, one for the 150 GHz band and one for the 220 GHz band. In the most recent test run a 144 pixel Al LeKID array was used for the 150 GHz band (Fig. 7A), developed by Cardiff, IRAM and Institute Néel. For the 220 GHz band a 256 pixel lens-antenna coupled array was used (Fig. 7B), developed by SRON/TU Delft. It uses a small twin slot antenna that is incorporated into the resonator itself to couple radiation from free space directly into the CPW resonator of the KID itself. The MKID CPW is made of NbTiN, with a gap frequency of 1.2 THz and radiation is absorbed in a short Al central line section close to the antenna, analog to the MUSIC design (see Fig. 6). This MKID array is coupled to a Si microlens array to create a high filling factor. A dedicated readout developed by the consortium is used to read out the array [38]. The tested NIKA instrument has a weak-source flux detectivity of 450 and 37 mJy $s^{1/2}$ for the 150 GHz and 220 GHz band respectively, which is above the photon noise limit of the sky, but for the 150 GHz band approaching the performance of

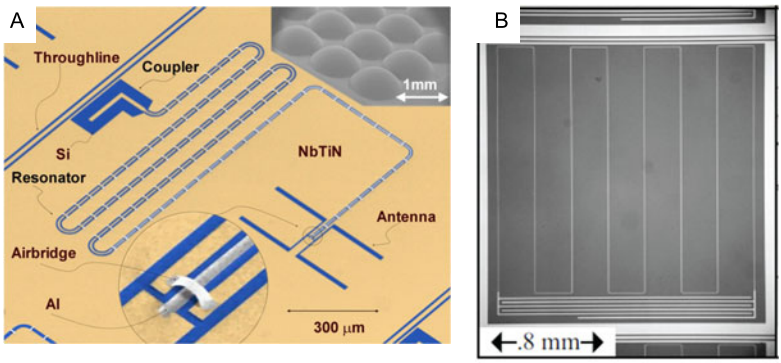

Fig. 7 (Color online) **A**: Direct antenna coupled $\lambda/4$ CPW resonator used for the 220 GHz band of NIKA. **B**: Al LeKID for the 150 GHz band of NIKA (from [36, 37])

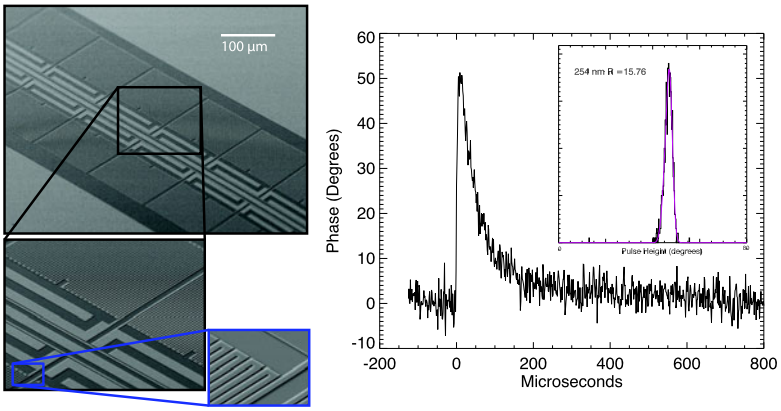

Fig. 8 (Color online) *Left*: Scanning electron micrograph of the TiN based optical lumped element KIDS used in ARCONS. *Right*: The typical phase response of a OLE MKID when illuminated with 254 nm photons. The *inset* shows actual data from an OLE MKID, consisting of a histogram of 5000 photons with an energy resolution $R = E/\delta dE = 16$. Reproduced from [40]

similar instruments [36, 37]. A similar dual color instrument, A-MKID, is being developed by a Dutch-German consortium, based upon the lens-antenna coupled KIDs [16] and a digital back-end developed by Max Planck institute in Bonn [39].

ARCONS is a near IR and optical camera developed by UCSB, Caltech and JPL developed for the Palomar 200″ telescope. The detectors for this instrument are optical lumped element KIDS (OLE-MKIDS) fabricated from TiN, in which the optical photons are absorbed directly into the meander of the LeKID. A micrograph of the devices is shown in Fig. 8. This offers a large advantage over more conventional strip detectors which suffer from quasiparticle trapping [41, 42]. An energy resolution $E/\delta E = 16$ was reported for these devices using 254 nm photons (see the right panel of Fig. 8). The instrument is currently tested for the first time.

Apart from these relatively mature instruments MKIDs have been demonstrated for several different applications, using different device geometries. KIDs developed for particle detection detect quasiparticles in a superconducting film created by the absorption of phonons from the absorption of high energetic particles in Si or Ge crystals. Cosmic ray detectors based upon LeKID devices on Si are proposed in Swenson et al. [43]. A dark mater detector based upon microstrip resonators on Si or Ge crystals with vacuum as dielectric has been proposed and tested by Daal et al. [45, 46] and another device using planar CPW technology for WIMP detection is proposed by Golwala et al. [47]. X-ray detection with MKIDs has been proposed using Ta strip detectors [44], but the Fano limit imposed by direct quasiparticle creation and quasiparticle trapping limit the energy resolution of such devices to less that 1000 for 5 keV photons, worse than TES detectors or magnetic calorimeters. Very recently X-ray detection by sensing high energy phonons has been proposed [48, 49]. MKIDs were also proposed to in-situ measure the permittivity of liquid He using Nb resonators [53].

Another very interesting recent development is the design and fabrication of on chip spectrometers based upon MKIDs. These devices use a broad band antenna and on-chip filtering structures to separate radiation in many ultra-narrow bands and couple each of these bands to a separate MKID [50, 51], taking the mm filtering concept from Music [33] further. A different approach is proposed by [52], where a stationary wave is spatially sampled by an array of MKIDs.

7 Conclusions

MKIDs development has increased significantly over the last few years. Several instruments are being developed and our understanding of the device operation has increased significantly. Several important subjects for near future developments remain: Our understanding of how MKIDs behave under significant loading is still not complete and photon noise limited performance of a full sub-mm instrument has yet to be demonstrated. A very interesting development are TiN based LeKIDs, which promise very simple and sensitive instruments for several applications. Much work remains to be done in fabrication and understanding these devices to be able to reach fundamental sensitivity limits with TiN. Al MKIDs have shown photon noise and generation-recombination noise limited performance, but the generation noise limited NEP is still a factor 10 too high for application in a space-borne spectrometer instrument with its optics cooled to 4 K. On-chip spectrometers in combination with background limited MKIDs are a very promising development toward such missions.

References

1. D.C. Mattis, J. Bardeen, Phys. Rev. **111**, 412 (1958)
2. R. Meservey, P.M. Tedrow, J. Appl. Phys. **40**, 2028 (1969)
3. D.G. McDonald, Appl. Phys. Lett. **50**, 775 (1987)
4. J. Zmuidzinas, B.A. Mazin, A. Vayonakis, P.K. Day, H.G. LeDuc, AIP Conf. Proc. **1**, 309–312 (2002)
5. A.V. Sergeev, V.V. Mitin, B.S. Karasik, Appl. Phys. Lett. **80**, 2002 (2002–2004)

6. P.K. Day, H.G. Leduc, B.A. Mazin, A. Vayonakis, J. Zmuidzinas, Nature **425**, 817 (2003)
7. A. Kozorezov, A. Volkov, J. Wigmore, A. Peacock, A. Poelaert, R. den Hartog, Phys. Rev. B, Condens. Matter Mater. Phys. **61**, 11807–11819 (2000)
8. S.B. Kaplan, C.C. Chi, D.N. Langenberg, J.J. Chang, S. Jafarey, D.J. Scalapino, Phys. Rev. B, Condens. Matter Mater. Phys. **14**, 4854 (1976)
9. C.M. Wilson, L. Frunzio, D. Prober, Phys. Rev. Lett. **87**, 067004 (2001)
10. C.M. Wilson, D. Prober, Phys. Rev. B, Condens. Matter Mater. Phys. **69**, 1–11 (2004)
11. P.J. de Visser, J.J.A. Baselmans, P. Diener, S.J.C. Yates, A. Endo, T.M. Klapwijk, Phys. Rev. Lett. **106**, 167004 (2011)
12. J. Baselmans, S. Yates, P. de Visser, These proceedings (2011)
13. P.J. de Visser, J.J.A. Baselmans, P. Diener, S.J.C. Yates, A. Endo, T.M. Klapwijk, J. Low Temp. Phys. (2012). doi:10.1007/s10909-012-0519-5
14. R.W. Boyd, Infrared Phys. **22**, 157–162 (1982)
15. J. Zmuidzinas, Ann. Rev. Cond. Matter Phys. (2011)
16. S.J.C. Yates, J.J.A. Baselmans, A. Endo, R.M.J. Janssen, L. Ferrari, P. Diener, A.M. Baryshev, Appl. Phys. Lett. **99**, 073505 (2011)
17. S.J.C. Yates, J.J.A. Baselmans, A. Endo, R.M.J. Janssen, L. Ferrari, P. Diener, A.M. Baryshev, These proceedings (2011)
18. H.G. Leduc et al., Appl. Phys. Lett. **97**, 102509 (2010)
19. M.R. Vissers, J. Gao, D.S. Wisbey, D.A. Hite, A.D. Corcoles, M. Steffen, D.P. Pappas, Appl. Phys. Lett. **97**, 232509 (2010)
20. J. Gao, J. Zmuidzinas, B.A. Mazin, H.G. Leduc, P.K. Day, Appl. Phys. Lett. **90**, 102507 (2007)
21. J. Gao, L.R. Vale, J.A.B. Mates, D.R. Schmidt, G.C. Hilton, K.D. Irwin, F. Mallet, K.W. Lehnert, H.G. Leduc, Appl. Phys. Lett. **98** (2011)
22. J.J.A. Baselmans, S.J.C. Yates, R. Barends, Y.J.Y. Lankwarden, J.R. Gao, H. Hoevers, T.M. Klapwijk, J. Low Temp. Phys. **151**, 524–529 (2008)
23. J. Martinis et al., Phys. Rev. Lett. **95**, 210503 (2005)
24. J. Gao et al., Appl. Phys. Lett. **92**, 212504 (2008)
25. R. Barends, H.L. Hortensius, T. Zijlstra, J.J.A. Baselmans, S.J.C. Yates, J.R. Gao, T.M. Klapwijk, Appl. Phys. Lett. **92**, 223502 (2008)
26. O. Noroozian, J. Gao, J. Zmuidzinas, H.G. Leduc, B.A. Mazin, AIP Conf. Proc. **1185**, 148–151 (2009)
27. R. Barends, N. Vercruyssen, A. Endo, P.J. de Visser, T. Zijlstra, T.M. Klapwijk, J.J.a. Baselmans, Appl. Phys. Lett. **97**, 033507 (2010)
28. S.J. Weber, K.W. Murch, D.H. Slichter, R. Vijay, I. Siddiqi, Appl. Phys. Lett. **98**, 172510 (2011)
29. B.A. Mazin et al., Appl. Phys. Lett. **96**, 102504 (2010)
30. B. Mazin, Microwave Kinetic Inductance Detectors. Ph.D. Thesis, California Institute of Technology (2004)
31. S. Doyle, P. Mauskopf, J. Naylon, a. Porch, C. Duncombe, J. Low Temp. Phys. **151**, 530–536 (2008)
32. A.-D. Brown, W.-T. Hsieh, S.H. Moseley, T.R. Stevenson, K. U-yen, E.J. Wollack, in *Proc. SPIE Astronomical Telescopes and Instrumentation*, vol. 7741 (2010), p. 77410P
33. P.R. Maloney et al., in *Proc. SPIE Astronomical Telescopes and Instrumentation*, vol. 7741 (2010), p. 77410F and references therein
34. P.R. Maloney et al., AIP Conf. Proc. **1185**, 176–179 (2009)
35. R. Duan et al., in *Proc. SPIE Astronomical Telescopes and Instrumentation*, vol. 7741 (2010), p. 77411V
36. A. Monfardini et al., Astron. Astrophys. **521**, A29 (2010)
37. A. Monfardini et al., Astrophys. J. Suppl. **194** (2011)
38. O. Bourrion, A. Bideaud, A. Benoit, A. Cruciani, A. Monfardini, M. Roesch, L. Swenson, C. Vescovi, arXiv:1102.1314 (2011)
39. S.J.C. Yates, A.M. Baryshev, J.J.A. Baselmans, B. Klein, R. Güsten, Appl. Phys. Lett. **95**, 042504 (2009)
40. B.A. Mazin, S. Mchugh, B. Bumble, D. Moore, J. Zmuidzinas, S. Barbara, Proc. SPIE **773518**, 773518P-1 (2010)
41. B.A. Mazin, M.E. Eckart, B. Bumble, S. Golwala, P.K. Day, J.S Gao, J. Zmuidzinas, J. Low Temp. Phys. **151**, 537–543 (2008)
42. D.C. Moore, B.A. Mazin, S. Golwala, B. Bumble, J. Gao, B.A. Young, Sean Mchugh, P.K. Day, H.G. Leduc, J. Zmuidzinas, AIP Conf. Proc. **1185** (2009)

43. L.J. Swenson, A. Cruciani, A. Benoit, M. Roesch, C.S. Yung, A. Bideaud, A. Monfardini, Appl. Phys. Lett. **96**, 263511 (2010)
44. B.A. Mazin, B. Bumble, P.K. Day, M.E. Eckart, S. Golwala, J. Zmuidzinas, F.A. Harrison, Appl. Phys. Lett. **89** (2006)
45. M. Daal, B. Sadoulet, J. Gao, J. Low Temp. Phys. **151**, 544–549 (2008)
46. M. Daal et al., These proceedings (2011)
47. S. Golwala, J. Gao, D. Moore, B. Mazin, M. Eckart, B. Bumble, P. Day, H.G. LeDuc, J. Zmuidzinas, J. Low Temp. Phys. **151**, 550–556 (2008)
48. A. Cruciani, L. Swenson, A. Monfardini, N. Boudou, M. Calvo, M. Roesch, These proceedings (2011)
49. D. Morre, S. Golwala, B. Bumble, B. Mazin, P. Day, H. LeDuc, J. Zmuidzinas, These proceedings (2011)
50. A. Endo, P. van der Werf, R.M.J. Janssen, P. de Visser, T.M. Klapwijk, J.J.A. Baselmans, L. Ferrari, A.M. Baryshev, S.J.C. Yates, arXiv:1107.3333 [astro-ph] (2011)
51. H. Moseley, W.-T. Hsieh, T. Stevenson, E. Wollack, A. Brown, D. Benford, J. Sadler, K. U-yen, N. Ehsan, J. Zmuidzinas, M. Bradford, These proceedings (2011)
52. N. Boudou, N. Boudou, N. Boudou, N. Boudou, N. Boudou, N. Boudou, J. Low Temp. Phys. (2012). doi:10.1007/s10909-012-0464-3
53. G.J. Grabovskij, L.J. Swenson, O. Buisson, C. Hoffmann, A. Monfardini, J.-C. Villégier, Appl. Phys. Lett. **93**, 134102 (2008)